



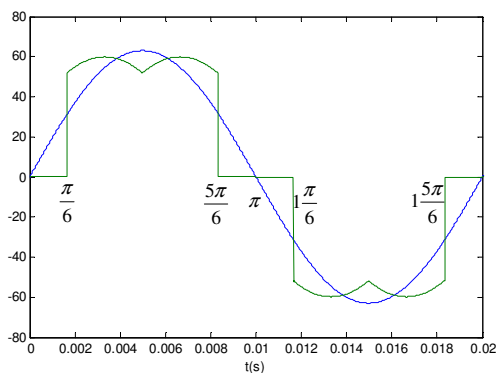


Table 1 Working phase of main and subordinate rectifier and formulas of  $I_a$ ,  $I_b$ ,  $I_c$  during a period

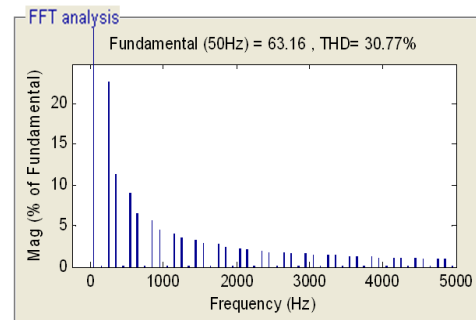
	$(0, \frac{\pi}{6})$	$(\frac{\pi}{6}, \frac{2\pi}{6})$	$(\frac{2\pi}{6}, \frac{3\pi}{6})$	$(\frac{3\pi}{6}, \frac{4\pi}{6})$	$(\frac{4\pi}{6}, \frac{5\pi}{6})$	$(\frac{5\pi}{6}, \frac{6\pi}{6})$
Working phase of main rectifier	BC	AC	AC	AB	AB	CB
Working phase of subordinate rectifier	AC	BC	AB	AC	CB	AB
$I_a$	$I_{aa}$	$I_{am}$	$I_{aa} + I_{am}$	$I_{aa} + I_{am}$	$I_{am}$	$I_{aa}$
$I_b$	$I_{bm}$	$I_{ba}$	$I_{ba}$	$I_{bm}$	$I_{bm} + I_{ba}$	$I_{bm} + I_{ba}$
$I_c$	$I_{cm} + I_{ca}$	$I_{cm} + I_{ca}$	$I_{cm}$	$I_{ca}$	$I_{ca}$	$I_{cm}$
	$(\frac{6\pi}{6}, \frac{7\pi}{6})$	$(\frac{7\pi}{6}, \frac{8\pi}{6})$	$(\frac{8\pi}{6}, \frac{9\pi}{6})$	$(\frac{9\pi}{6}, \frac{10\pi}{6})$	$(\frac{10\pi}{6}, \frac{11\pi}{6})$	$(\frac{11\pi}{6}, \frac{12\pi}{6})$
Working phase of main rectifier	CB	CA	CA	BA	BA	BC
Working phase of subordinate rectifier	CA	CB	BA	CA	BC	BA
$I_a$	$I_{aa}$	$I_{am}$	$I_{aa} + I_{am}$	$I_{aa} + I_{am}$	$I_{am}$	$I_{aa}$
$I_b$	$I_{bm}$	$I_{ba}$	$I_{ba}$	$I_{bm}$	$I_{bm} + I_{ba}$	$I_{bm} + I_{ba}$
$I_c$	$I_{cm} + I_{ca}$	$I_{cm} + I_{ca}$	$I_{cm}$	$I_{ca}$	$I_{ca}$	$I_{cm}$

The current waveform  $I_a$  is shown in Fig.3. The missing current during  $(0, \pi/6)$ ,  $(5\pi/6, 7\pi/6)$ ,  $(11\pi/6, 2\pi)$  makes  $I_a$  distort. If the missing current is compensated, the harmonic of  $I_a$  will reduce obviously. So the bi-boost crossing converter should be controlled to compensate the missing current during  $(0, \pi/6)$ ,  $(5\pi/6, 7\pi/6)$ ,  $(11\pi/6, 2\pi)$  and improve the current during  $(\pi/6, 5\pi/6)$ ,  $(7\pi/6, 11\pi/6)$ . It's the same with phase B and C.

Based on the above analysis,  $I_r$  is in phase with  $V_a$ , which is presented in Fig.4.



(a) The waveform of phase current  $I_a$



(b) The frequency spectrum of  $I_a$

Fig.3 Phase current waveforms and frequency spectrum of three-phase uncontrolled rectifier without capacitor

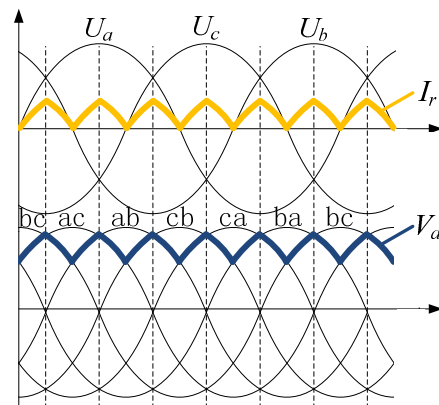


Fig.4 Ideal waveforms of  $I_r$  and  $V_a$

### 3 Harmonic Analysis of Input Current

Supposing the peak value of phase voltage is  $V$  and the output power is  $P$ . The following harmonic analysis is based on the constant power load (just like DC-DC converter).

Three phase voltages are

$$\begin{cases} U_a = V \sin(\omega t) \\ U_b = V \sin(\omega t + 2\pi/3) \\ U_c = V \sin(\omega t + 4\pi/3) \end{cases} \quad (5)$$

If the power factor is unity, three phase input currents are

$$\begin{cases} I_a = k \sin(\omega t) \\ I_b = k \sin(\omega t + 2\pi/3) \\ I_c = k \sin(\omega t + 4\pi/3) \end{cases} \quad (6)$$

For the output power  $P$

$$P = U_a I_a + U_b I_b + U_c I_c = 1.5V k, \quad k = \frac{P}{1.5V} \quad (7)$$

So

$$\begin{cases} I_a = \frac{P}{1.5V} \sin(\omega t) \\ I_b = \frac{P}{1.5V} \sin(\omega t + 2\pi/3) \\ I_c = \frac{P}{1.5V} \sin(\omega t + 4\pi/3) \end{cases} \quad (8)$$

If the filter capacitors  $C_m$  and  $C_a$  are ignored and the switching frequency can be as high as possible, the output voltage of subordinate rectifier is close to six-pulse. Since the frequency of  $I_r$  is six times as power frequency, the current harmonic is only analyzed during interval  $(0, \pi/3)$ . The relationship of phase currents is shown in Fig.5 during this interval. The reference direction of input current has been marked in Fig.1.

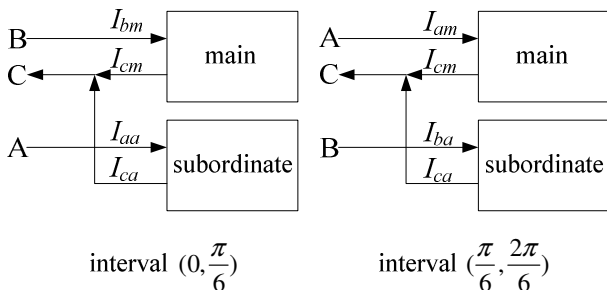


Fig.5 Relationship of phase currents during  $(0, \pi/3)$

(1) Interval  $(0, \pi/6)$

The working phases of main rectifier are phase B and C, while phase A and C are the working phases of subordinate rectifier.

$$V_0 = V_{bc} = \sqrt{3}V \sin(\omega t + \pi/2) \quad (9)$$

$$V_a = V_{ac} = \sqrt{3}V \sin(\omega t + \pi/6) \quad (10)$$

In order to compensate the missing current and achieve unity power factor during this interval,

$$I_a = I_{aa} = \frac{P}{1.5V} \sin(\omega t) \quad (11)$$

Due to the power conservation principle, the relationship between  $I_r$  and  $I_s$  is

$$I_s = \frac{V_a I_r}{V_0} = \frac{P}{\sqrt{3}V} \times \frac{\sin(\omega t) \sin(\omega t + \frac{\pi}{6})}{\sin(\frac{\pi}{3}) \sin(\omega t + \frac{\pi}{2})} \quad (12)$$

$$I_b = I_{bm} = \frac{P}{V_0} - I_s = \frac{P}{1.5V} \sin(\omega t + \frac{2}{3}\pi) \quad (13)$$

$$I_c = I_{cm} + I_{ca} = -I_{bm} - I_{aa} = \frac{P}{1.5V} \sin(\omega t - \frac{2\pi}{3}) \quad (14)$$

(2) Interval  $(\pi/6, \pi/3)$

The working phases of main rectifier are phase A and C, while phase B and C are working phases of subordinate rectifier.

$$V_0 = V_{ac} = \sqrt{3}V \sin(\omega t + \frac{\pi}{6}) \quad (15)$$

$$V_a = V_{bc} = \sqrt{3}V \sin(\omega t + \frac{\pi}{2}) \quad (16)$$

In order to compensate the missing current during this interval,

$$I_b = I_{ba} = \frac{P}{1.5V} \sin(\omega t + \frac{2\pi}{3}) \quad (17)$$

Due to the power conservation principle, the relationship between  $I_r$  and  $I_s$  is

$$I_s = \frac{V_a I_r}{V_0} = \frac{P}{\sqrt{3}V} \times \frac{\sin(\omega t + \frac{2\pi}{3}) \sin(\omega t + \frac{\pi}{2})}{\sin(\frac{\pi}{3}) \sin(\omega t + \frac{\pi}{6})} \quad (18)$$

$$I_a = I_{am} = \frac{P}{V_0} - I_s = \frac{P}{1.5V} \sin(\omega t) \quad (19)$$

$$I_c = I_{cm} + I_{ca} = -I_{am} - I_{ba} = \frac{P}{1.5V} \sin(\omega t - \frac{2\pi}{3}) \quad (20)$$

The formula of input current is the same during the other intervals. According to the analysis above, when (11) and (17) is satisfied,  $I_a, I_b, I_c$  will be

sinusoidal and the power factor will be unity if the load is constant-power, the filter capacitors  $C_m$  and  $C_a$  are ignored and the switching frequency is as high as possible.

Actually the switching frequency can't be as high as possible, so the filter capacitors  $C_a$  and  $C_m$  should be considered. The formulae of phase A current  $I_a$  are shown as follows.

Intervals  $(0, \pi/6)$ ,  $(\pi, 7\pi/6)$

$$I_a = \frac{P}{1.5V} \sin(\omega t) + \sqrt{3}V \cdot \omega C_a \cos(\omega t + \frac{\pi}{6}) \quad (21)$$

Intervals  $(\pi/6, \pi/3)$ ,  $(7\pi/6, 8\pi/6)$

$$I_a = \frac{P}{1.5V} \sin(\omega t) + \sqrt{3}V \cdot \omega C_m \cos(\omega t + \frac{\pi}{6}) \quad (22)$$

Intervals  $(\pi/3, \pi/2)$ ,  $(4\pi/3, 3\pi/2)$

$$I_a = \frac{P}{1.5V} \sin(\omega t) + \sqrt{3}V[\omega C_m \cos(\omega t + \frac{\pi}{6}) + \omega C_a \cos(\omega t - \frac{\pi}{6})] \quad (23)$$

Intervals  $(\pi/2, 2\pi/3)$ ,  $(3\pi/2, 5\pi/3)$

$$I_a = \frac{P}{1.5V} \sin(\omega t) + \sqrt{3}V[\omega C_m \cos(\omega t - \frac{\pi}{6}) + \omega C_a \cos(\omega t + \frac{\pi}{6})] \quad (24)$$

Intervals  $(2\pi/3, 5\pi/6)$ ,  $(5\pi/3, 11\pi/6)$

$$I_a = \frac{P}{1.5V} \sin(\omega t) + \sqrt{3}V \cdot \omega C_m \cos(\omega t - \frac{\pi}{6}) \quad (25)$$

Intervals  $(5\pi/6, \pi)$ ,  $(11\pi/6, 2\pi)$

$$I_a = \frac{P}{1.5V} \sin(\omega t) + \sqrt{3}V \cdot \omega C_a \cos(\omega t - \frac{\pi}{6}) \quad (26)$$

It's concluded that the harmonic current is concerned with gross power  $P$ , peak value of phase voltage  $V$ , angular frequency  $\omega$  and filter capacitors  $C_m$  and  $C_a$  if the filter capacitors  $C_a$  and  $C_m$  are considered.

### 4 Principle of Control System

It is only needed to control the switch  $S_a$ ,  $S_b$ ,  $S_c$ ,  $K_1$  and  $K_2$  to achieve ideal power factor and low harmonic current. The system control scheme of subordinate rectifier is shown in Fig.6. In order to achieve ideal power factor and low harmonic current, the average value of  $I_{s1}$ ,  $I_{s2}$  and the waveforms of  $I_{r+}$ ,  $I_{r-}$  should be controlled by

detecting the input current  $I_{r+}$  and  $I_{r-}$ , output current  $I_{s1}$  and  $I_{s2}$  and three phase voltages.

The time sequence of  $S_a$ ,  $S_b$  and  $S_c$  which is decided by the phase voltage is shown in Fig.2. Commonly the AC-DC switched converter has three control methods: peak current control, hysteresis current control and average current control. The advantages of hysteresis current control are proposed as follows: simple control, quick dynamic response of current, excellent disturbances attenuation performances and robustness. So the hysteresis current control scheme which is represented in Fig.7 has been chosen for this novel APFC topology. The values of  $I_{r+}$  and  $I_{s1}$  are the current feedbacks for  $K_1$ , while the values of  $I_{r-}$  and  $I_{s2}$  are the current feedbacks for  $K_2$ . So  $K_1$  and  $K_2$  are controlled independently, but both of them choose  $I_{r(wave)}$  as reference phase current. The circulation will be avoided by controlling  $K_1$  and  $K_2$  independently.

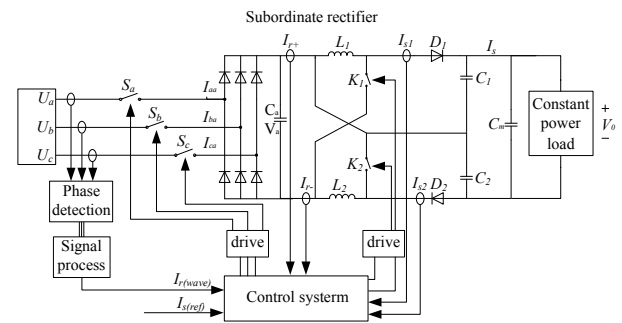


Fig.6 System control scheme of three-phase parallel PFC with feed-forward compensation

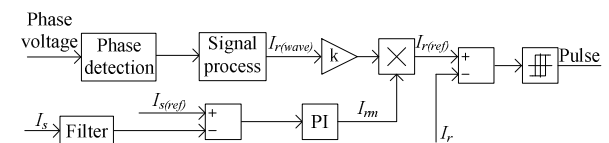


Fig.7 Hysteresis current control scheme of three-phase parallel PFC with feed-forward compensation

The control scheme to implement three-phase parallel PFC with feed-forward compensation should focus on two points:

1) The load power is constant;

2) Compensate the missing current in zero crossing interval of each phase and keep the power factor unity. For example, during  $(0, \pi/6)$ ,  $I_{r+} = I_{r-} = P \sin(\omega t) / 1.5V$ .

The main rectifier which is a three-phase uncontrolled rectifier is equivalent as a voltage

source, while the subordinate rectifier whose output current is controlled is equivalent as a current source. The output voltage of this novel APFC topology is equal to the voltage of the equivalent voltage source. If the load power is constant, the load current  $I_0$  will be constant. The missing current can be compensated by controlling  $I_s$  and  $I_r$ .

The power of subordinate rectifier is

$$P_s = \frac{6}{\pi} \int_0^{\frac{\pi}{6}} \frac{P}{1.5V} \sin(\omega t) \cdot \sqrt{3}V \sin(\omega t + \frac{\pi}{6}) d\omega t$$

$$= V_m \times I_s = 0.224P \quad (27)$$

The total output power is  $P$ , and the power of main rectifier is

$$P_m = V_m \times I_m = P - 0.224P = 0.776P \quad (28)$$

According to (27) and (28)

$$\frac{I_m}{I_s} = \frac{97}{28} \quad (29)$$

If (29) is valid in this system and  $I_r$  is able to track the phase of  $I_{r(wave)}$ , ideal power factor and low harmonic current will be achieved.

The relationship between  $I_{r(wave)}$  and  $V_a$  is shown in Fig.4.  $I_{r(wave)}$  is decided by phase voltage.  $I_{s(ref)}$  is the reference current of outer current loop. According to (29),  $I_{s(ref)}=28I_m/97$ . The reference current of inductance  $I_{r(ref)}$  is the product of  $kI_{r(wave)}$  and the output of the PI controller of the current outer loop. The principle of hysteresis current control is shown in Fig.8. The upper limit of hysteresis loop is defined as  $I_{r(ref)} + \Delta h$  and the lower limit is  $I_{r(ref)} - \Delta h$ . If  $I_r > I_{r(ref)} + \Delta h$ , switch will be off and the inductance current will decrease, otherwise switch will be on and the inductance current will increase. The inductance current fluctuate near the reference current  $I_{r(ref)}$  by controlling  $K_1$  and  $K_2$ . How to choose  $\Delta h$  for the control system is important, because it's concerned with current harmonic. In order to improve the switching characteristic of  $K_1$  and  $K_2$ , the sample value of inductance current should be filtered.

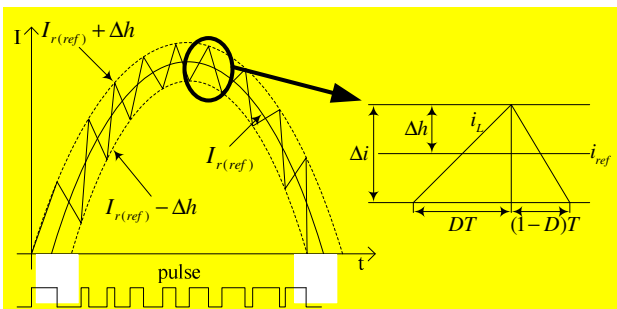


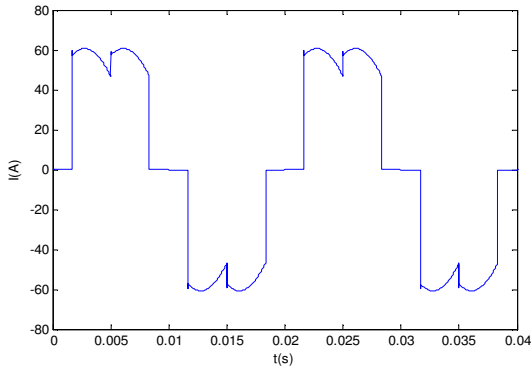
Fig.8 Principle of hysteresis current control

## 5 Simulation Results

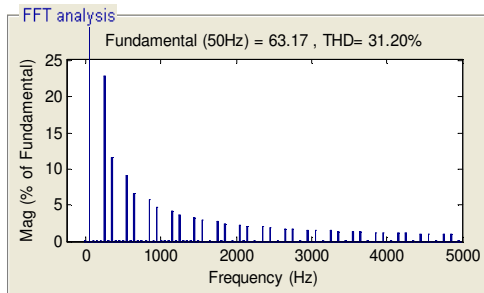
The MATLAB/Simulink simulation model consists of a three phase voltage source (with peak phase voltage  $V=311V$  and  $f=50Hz$ ) and a three-phase parallel PFC with feed-forward compensation. The output power is 30 KW, and the maximum switching frequency is 20 KHz. For the inductors  $L$ , we have adopted the value of 0.5mH. The filter capacitor  $C_m$  is 40uF, and  $C_a$  is 20uF. For the outer current loop of control system, the scale factor  $K_p=0.015$  and the integral factor  $K_i=5$ . The scale factor of phase control loop  $K$  is 0.1, and the hysteresis width  $\Delta h$  is 3.

The phase current  $I_a$  of normal three-phase uncontrolled rectifier, theoretical model and simulation model with hysteresis current control are presented in Fig.9, Fig.10 and Fig.11 respectively. With the filter whose cut-off frequency is 5 KHz, the frequency spectrum of  $I_a$  is shown in Fig.12. From theoretical model, the THD (Total Harmonic Distortion) of  $I_a$  is 4.65%, while the THD of  $I_a$  is 10.84% from simulation model. Compared with 31.2% of normal three-phase uncontrolled rectifier, THD has reduced obviously. The reason why the THD of simulation is higher than the theoretical THD is as follows: the theoretical  $I_s$  and  $I_m$  are continuous, while  $I_s$  and  $I_m$  from the simulation model are pulsing, which will generate additional higher harmonic. So from the simulation model, the THD of  $I_a$  reduces to 5.86% with the filter whose cut-off frequency is 5 KHz.

The current waveforms of  $I_{aa}$ ,  $I_{am}$ ,  $I_a$  are shown in Fig.13 and the current waveforms of  $I_a$ ,  $I_b$ ,  $I_c$  are shown in Fig.14.  $I_{aa}$  is the compensation of the missing current. In Fig.13,  $I_a$  is the sum of  $I_{aa}$  and  $I_{am}$ . The input and output voltage waveforms of bi-boost crossing converter are shown in Fig.15 and 16. The input current waveforms  $I_{r+}$ ,  $I_{r-}$  of bi-boost crossing converter are shown in Fig.17 (a) and (b).  $V_a$ ,  $I_{r+}$ ,  $I_{r-}$  from simulation model are coincide with the theoretical results which are shown in Fig.4 and the load voltage  $V_0$  which is equal to the output voltage of main rectifier is six-pulse during a period. Fig.18 shows the voltage and current waveforms of phase A. As is shown in Fig.18, the power factor is 0.9932, which verify the feasibility of this novel APFC topology. Fig.19 shows the waveform of output power, which verifies the premise that the load power keeps constant in the simulation model. In Fig.20, Fig.21and Fig.22, the current stress of switch  $K_1$  and  $K_2$  is half of the one of normal boost converter, the voltage stress of switch  $K_1$  and  $K_2$  is  $1/(1+D)$  of the one of normal boost converter, which is coincide with the analysis mentioned in section 2.

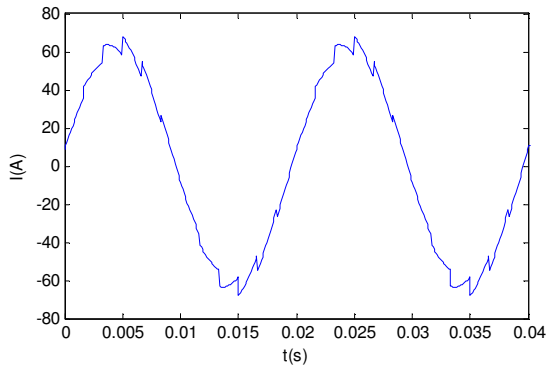


(a) The waveform of phase current  $I_a$

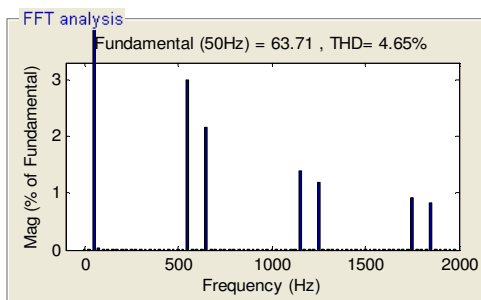


(b) The frequency spectrum of  $I_a$

Fig.9  $I_a$  and frequency spectrum of normal three-phase uncontrolled rectifier

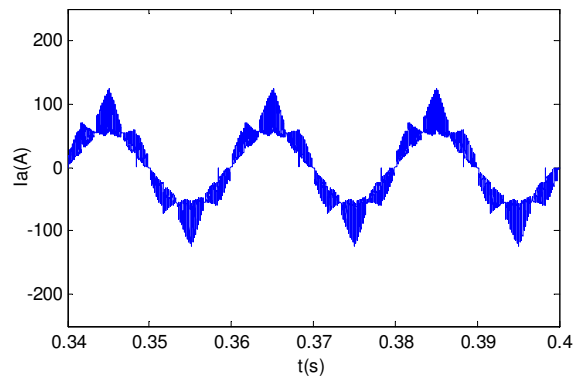


(a) The waveform of phase current  $I_a$

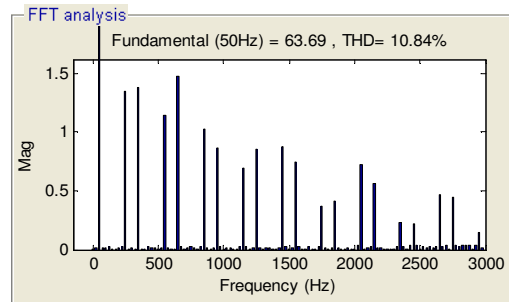


(b) The frequency spectrum of  $I_a$

Fig.10  $I_a$  and frequency spectrum from theoretical model under hysteresis current control

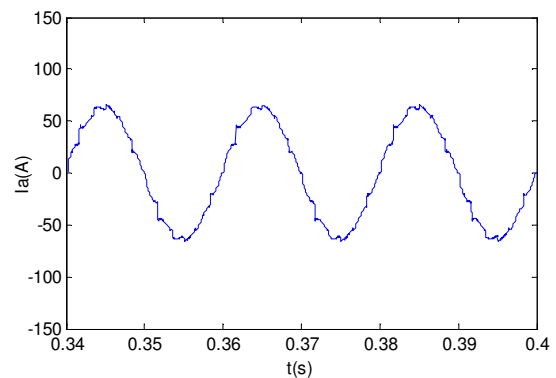


(a) The waveform of phase current  $I_a$

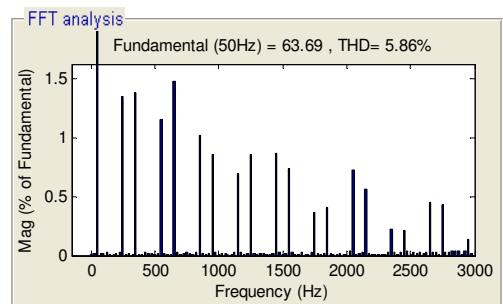


(b) The frequency spectrum of  $I_a$

Fig.11  $I_a$  and frequency spectrum from simulation model under hysteresis current control



(a) The waveform of phase current  $I_a$



(b) The frequency spectrum of  $I_a$

Fig.12  $I_a$  and frequency spectrum from simulation model with filter under hysteresis current control

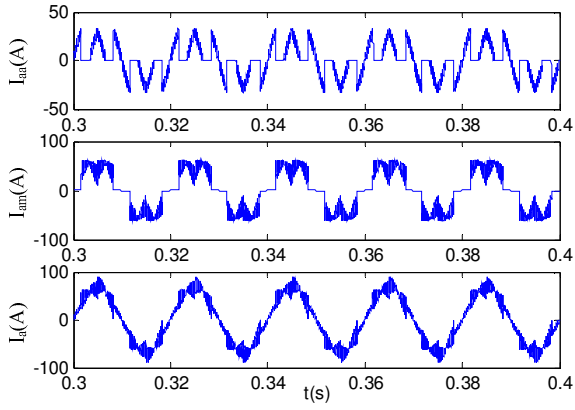


Fig.13 Current waveforms of  $I_{aa}$ ,  $I_{am}$ ,  $I_a$

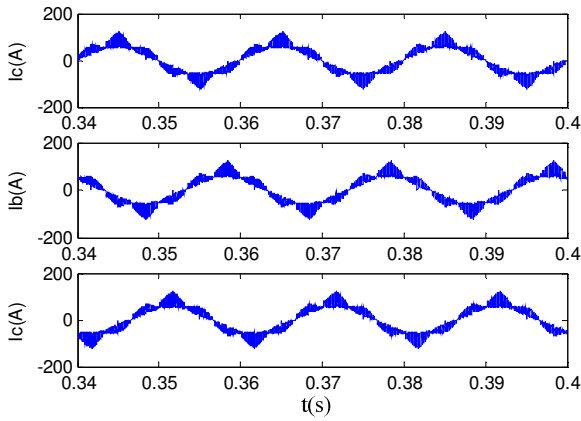


Fig.14 Current waveforms of  $I_a$ ,  $I_b$ ,  $I_c$

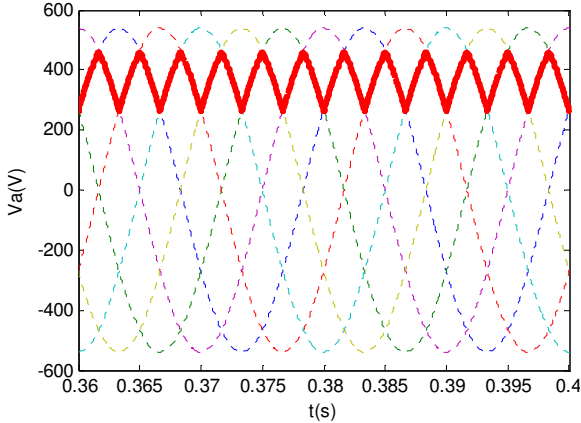


Fig.15 Voltage waveform of  $V_a$

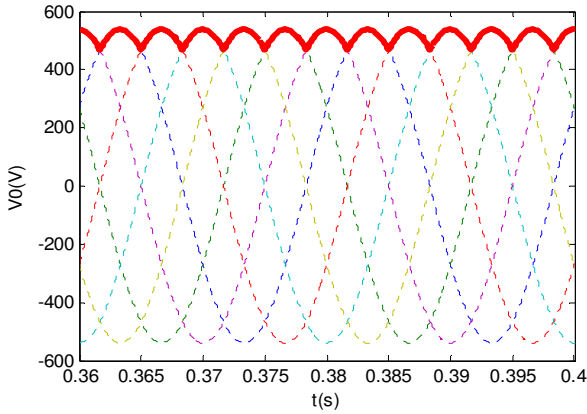
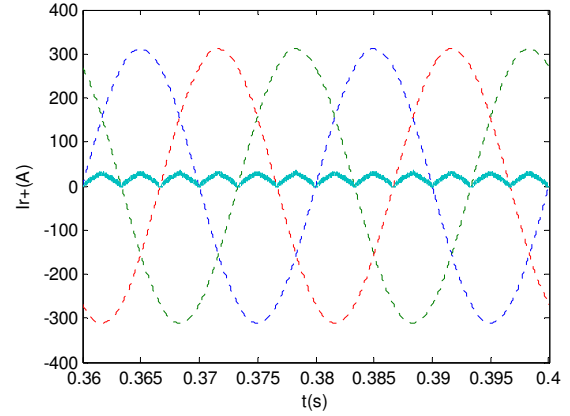
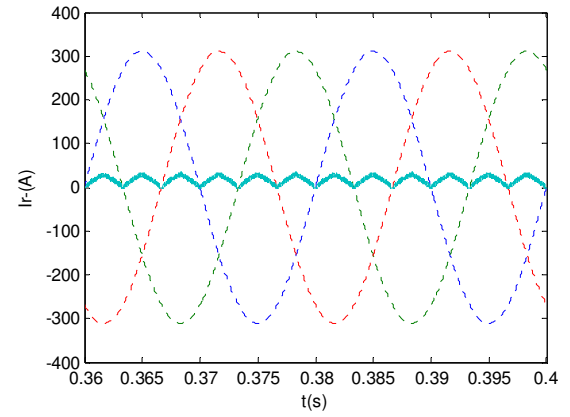


Fig.16 Voltage waveform of  $V_0$



(a) Current waveform of  $I_{r+}$



(b) Current waveform of  $I_{r-}$

Fig.17 Input current waveform of Boost circuit

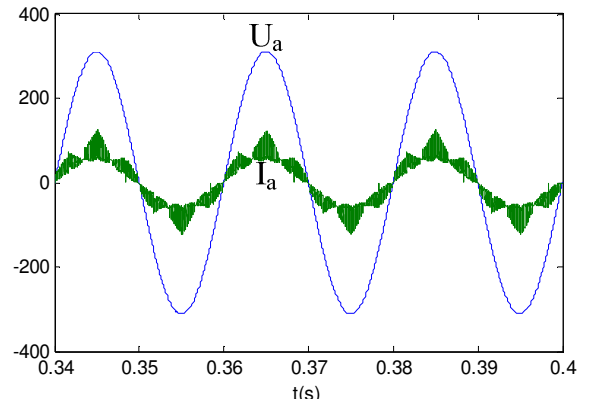


Fig.18 Voltage and current waveforms of phase A

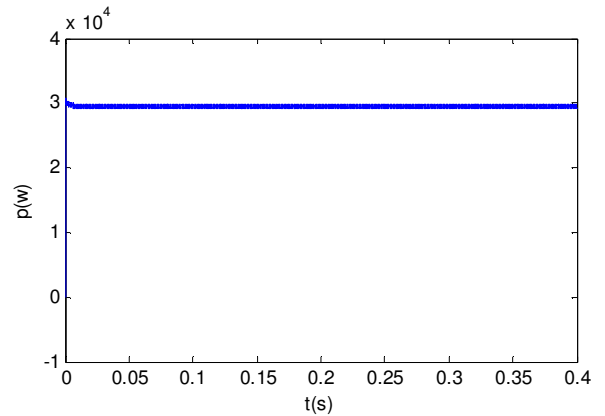
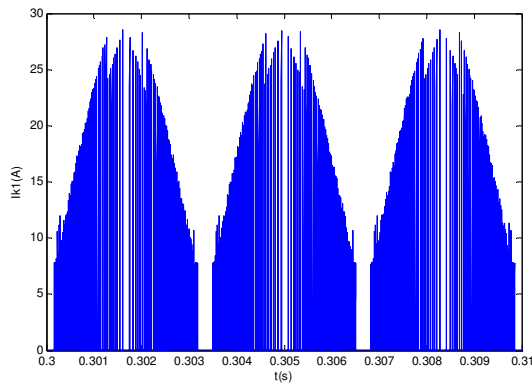
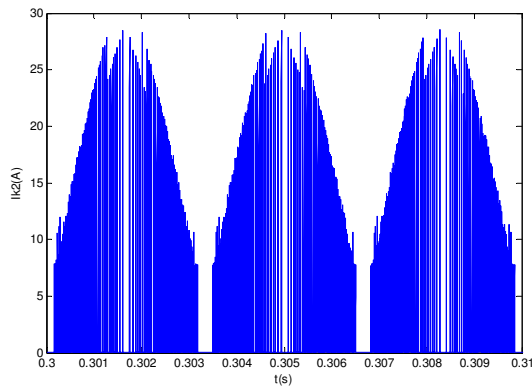


Fig.19 Waveform of output power





(a) Current stress of switch  $K_1$



(b) Current stress of switch  $K_2$

Fig.20 Current stress of switch of bi-boost crossing converter

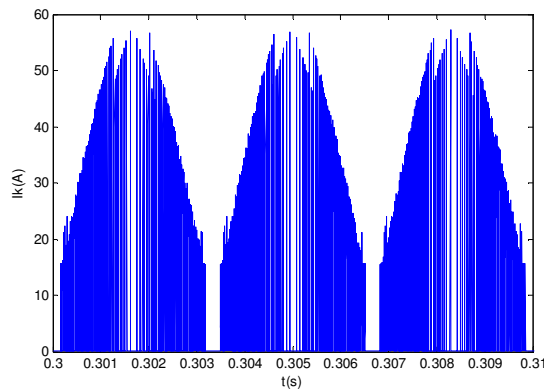
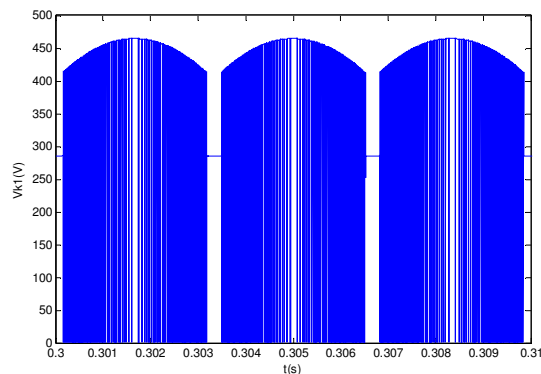
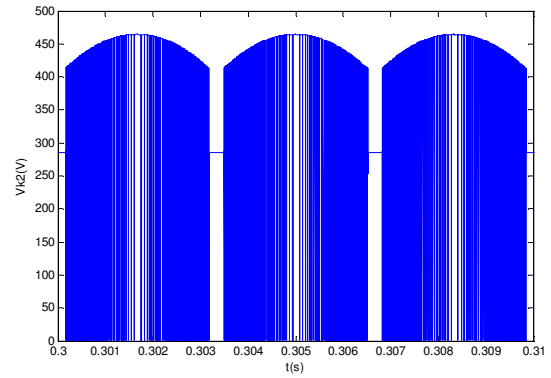


Fig.21 Current stress of switch of normal boost converter



(a) Voltage stress of switch  $K_1$



(b) Voltage stress of switch  $K_2$

Fig.22 Voltage stress of switch

## 6 Conclusion

The novel three-phase PFC topology cooperated with the hysteresis control technique has been proposed. It can stabilize the six-pulse dc output voltage, compensate the missing current during intervals  $(0, \pi/6)$ ,  $(5\pi/6, 7\pi/6)$ ,  $(11\pi/6, 2\pi)$  in a period and improve the other two phase current waveforms during the same interval. The theoretical analysis and the simulation results have proved the merits of small current THD and high power factor. However, when the load power has been changed heavily, the power factor and current THD will get worse, and the DC voltage is not adjustable. Approximately twenty percent of power goes through the boost converter and the bi-boost crossing converter can reduce the voltage and current stress of switch. Therefore, the lower power components can be chosen, which reduce the cost and improve the efficiency of the system. The novel APFC topology is suitable for the applications as follows:

- 1) Strict with power factor;
- 2) Output power is constant.

In total, the novel APFC topology has wide application prospects.

### References:

- [1] Zhang Zheyu, Zou Xudong, Wu Zhenxing et al., *Analysis on Harmonic Current of Three-phase Bridge Uncontrolled Rectifier*, IEEE Power and Energy Engineering Conference, Wuhan, China, 2010, pp.1-4.
- [2] Sakui, M., Fujita, H., Shioya, M., *A method for calculating harmonic currents of a three-phase bridge uncontrolled rectifier with DC filter*, IEEE Transactions on Industrial Electronics, Vol.36, No.3, 1999, pp.434-440.
- [3] Li Mingshui, Wan Jianru, Li Guangye et al,

*Research on power feedforward control strategy of PWM rectifier*, Power Electronics Systems and Applications, Tianjin, China, 2011, pp.1-6.

- [4] Chen Zhong, Zhu Yin-yu, Luo Ying-peng, *Three-Phase Rectifier With Near-Sinusoidal Input Currents and LC Filters Connected on the AC Side*, Transactions of China Electrotechnical Society, Vol.24, No.11, 2009, pp.108-113.
- [5] Chen Zhong, Zhu Yin-yu, Qiu Yan, et al, *Analysis and Design of Three-phase Rectifier With Near-sinusoidal Input Currents*, Proceedings of the CSEE, Vol.29, No.36, 2009, pp.29-34.
- [6] Burgos R P, Uan-Zo-li A, Lacaux F, et al, *Analysis of new step-up and step-down 18-pulse direct asymmetric autotransformer rectifiers*, IEEE Industry Applications Conference, Hong Kong, China, Vol.1, 2005, pp.145-152.
- [7] Chen Peng, Li Xiaofan, Xiong Zhaochun, et al, *A 12-pulse rectifier with an auxiliary circuit*, Proceedings of the CSEE, Vol.26, No.23, 2006, pp.163-166.
- [8] Singh B, Bhuvaneswari G, Garg V, *T-connected autotransformer-based 24-pulse AC-DC converter for variable frequency induction motor drives*, IEEE Transaction on Energy Conversion, Vol.21, No.3, 2006, pp.663-672.
- [9] Wang Zhaoan, Yang Jun, Liu Jinjun, et al, *Harmonic suppression and Reactive power compensation*, Beijing: Machine Press, 2005.
- [10] Divya, E., Gnanavadivel, J.. *Harmonic elimination in three phase PWM rectifier using FPGA control*, Emerging Trends in Electrical and Computer Technology Conference, Sivakasi, India, 2011, pp.436-441.
- [11] Hyunjae Yoo, Kim, J.-H., Seung-Ki Sul, *Sensorless Operation of a PWM Rectifier for a Distributed Generation*, IEEE Transactions on Power Electronics, Vol.22, No.3, 2007, pp.1014-1018.
- [12] Dae-Woong Chung, Seung-Ki Sul., *Minimum-loss strategy for three-phase PWM rectifier*, IEEE Transactions on Industrial Electronics, Vol.46, No.3, 1999, pp.517-526.
- [13] Y.F. Wang, *Boost converter with lower inter-phase rectifier parallel compensating three-phase power factor correction*, PCT/CN/02/00828.
- [14] Y.F. Wang, Bingxin Wang, Zian Zhu, *A Voltage-Adjustable Three-Phase Rectifier with Constant Power Flow*, Applied Power Electronics Conference and Exposition, 2008, pp.1372-1377.
- [15] Y.F. Wang, *Blocked Phase Current Patching Three-phase Rectifier and Motor Driver with Energy Feedback*, PCIM China, 2009, pp.168-173.
- [16] Y.F. Wang, *Three-phase parallel PFC with feed-forward compensation*: China, 01140014.5. 2003-05-28.
- [17] Yi. Li, *DC-DC Circuit with symmetrical crossing structure*: China, 101867314A. 2010-10-20.